



| | |
|------------------|--|
| Title | Counterpropagating Gradients of Antibacterial and Antifouling Polymer Brushes |
| Author(s) | Ko, Yeongun; Truong, Vi Khanh; Woo, Sun Young; Dickey, Michael D.; Hsiao, Lilian; Genzer, Jan |
| Citation | Biomacromolecules, 23(1), 424-430 https://doi.org/10.1021/acs.biomac.1c01386 |
| Issue Date | 2022-01-10 |
| Doc URL | http://hdl.handle.net/2115/88169 |
| Rights | This document is the Accepted Manuscript version of a Published Work that appeared in final form in Biomacromolecules, copyright © American Chemical Society after peer review and technical editing by the publisher. To access the final edited and published work see https://pubs.acs.org/articlesonrequest/AOR-HCKVXUIEBKGDQPQV8UUPB . |
| Type | article (author version) |
| File Information | Biomacromolecules_23(1)_424-430.pdf |



[Instructions for use](#)

Counter-propagating gradients of antibacterial and antifouling polymer brushes

Yeongun Ko^{1,†}, Vi Khanh Truong^{1,2}, Sun Young Woo¹, Michael D. Dickey¹, Lilian Hsiao¹,
Jan Genzer^{1,3,*}

¹ Department of Chemical and Biomolecular Engineering
North Carolina State University
Raleigh, NC 27695-7905, USA

² Nanobiotechnology Laboratory, School of Science
RMIT University
Melbourne, VIC 3000, Australia

³ Global Station for Soft Matter, Global Institution for Collaborative Research and Education
(GI-CoRE)
Hokkaido University
Hokkaido 060-0808, Japan

Abstract

We report on the formation of counter-propagating density gradients in poly([2-dimethylaminoethyl] methacrylate) (PDMAEMA) brushes featuring spatially varying quaternized and betainized units. Starting with PDMAEMA brushes with constant grafting density and degree of polymerization, we first generate a density gradient of quaternized units by directional vapor reaction involving methyl iodide. The unreacted DMAEMA units are then betainized through gaseous phase betainization with 1,3 propanesultone. The gas reaction of PDMAEMA with 1,3 propanesultone eliminates the formation of byproducts present in liquid phase modification. We use the counter-propagating density gradients of quaternized and betainized PDMAEMA brushes in antibacterial and antifouling studies. Completely quaternized and betainized brushes exhibited antibacterial and antifouling behavior. Samples containing 12% of quaternized and 85% of betainized units acted simultaneously as antibacterial and antifouling surfaces.

[†] Present address: Department of Chemical Engineering, University of Michigan, Ann Arbor, MI 48109-2800

* Corresponding author: jgenzer@ncsu.edu

Introduction

Polymeric coatings have been employed extensively in various applications, including adhesive layers, low friction surfaces, antifouling materials, responsive surfaces, colloidal stabilizers, *etc.*¹⁻³ Polymers offer higher versatility to tune the physical and chemical properties of surfaces than small-molecule modifiers (*e.g.*, organosilane coupling agents).^{4,5} Specifically, surface-grafted polymer assemblies (SGPA) generate stable coatings on the surface due to chemical covalent bonds.^{6,7} To obtain a high grafting density of polymer chains (number of chains per unit area, $1/\text{nm}^2$), one often uses the "grafting-from" method via surface-initiated atom transfer radical polymerization (SI-ATRP).^{7,8} Varying the grafting density, chain length, chain topology, and functional groups of repeat units in SGPA enables fine control of the properties of surfaces.^{9,10}

Post-polymerization modification (PPM) is a feasible alternative to a direct polymerization of functional monomers.¹¹⁻¹³ PPM alleviates inherent difficulties found in the direct polymerization of functional monomers.¹⁴ Because PPM does not alter the density and molecular weight of the parent polymers, it allows the direct characterization of a degree of modification and reaction kinetics.¹⁵⁻¹⁷ This point is beneficial for polymer brushes.¹⁸ Under the constant grafting density and degree of polymerization, any changes of physicochemical properties such as dry thickness or a refractive index after PPM modifications can be correlated with the extent of PPM reaction.^{16,19} For example, the exposure of poly([2-dimethylaminoethyl] methacrylate) (PDMAEMA) brushes to methyl iodide (MI) results in the rapid formation of quaternized PDMAEMA (qPDMAEMA).¹⁷ Through the quaternization, the modified repeat units carry complete positive charges with iodide counterions. The degree of quaternization can be characterized by elemental analysis, FTIR-ATR, and ellipsometry.

Another advantage of PPM is that it enables spatial control of the degree of functionality. For instance, a series of charge density gradients in PDMAEMA brushes was generated by diffusion of MI in the gaseous phase and reaction within the PDMAEMA brush.¹⁷ Only the charge densities were varied across the sample, while the degree of polymerization and the grafting densities remained constant. The gradient width and height could be tuned by changing the concentration of reagent or reaction time. Gradients in chemical or physical properties in films enable systematic investigation of a particular phenomenon of interest, thereby minimizing experimental error deviations and time-consuming sample preparation while allowing a comprehensive and systematic evaluation of sample attributes.²⁰⁻²²

Betainization, another modification of the tertiary amines in the PDMAEMA, generates a polyzwitterion containing negative and positive charges in their repeat units.²³ Polyzwitterionic brushes could be formed through either direct polymerization or PPM. In this work, we use PPM to create polyzwitterionic brushes via gaseous phase modification of parent PDMAEMA brushes with 1,3-propanesultone (P-S). In solution, P-S can hydrolyze to produce 3-ethoxy-propane-1-sulfonic acid, prohibiting betainization by protonating tertiary amines in PDMAEMA.²⁴ We will discuss that the gaseous phase modification avoids the generation of the undesired product. We provide details about the reaction kinetics as a function of reaction time and the concentration of P-S.

Charge-bearing polymers play a pivotal role in controlling the interfacial interactions between synthetic and biological species. Specifically, the positively-charged PDMAEMA exhibits antibacterial properties against gram-positive and gram-negative bacteria.²⁵ The qPDMAEMA acted similarly to other cationic biocides, attaching directly to bacteria, diffusing through the cell wall, disrupting the cytoplasmic membrane, and killing the bacteria. Polyzwitterions resist non-specific protein adsorption on surfaces.²⁶⁻³⁰ Thus, the polyzwitterionic brushes have often been studied as antifouling surfaces. Here, we developed counter-propagating gradients (CPG) of quaternized and betainized units in the PDMAEMA brushes through the quaternization gradient followed by betainization of unmodified repeat units. We carry out both PPM reactions in the gaseous phase.^{17,31,32} MI and P-S dissolved in ethanol solution are used as quaternization and betainization reagents.³³ We use the CPG surfaces to study simultaneously antibacterial and anti-fouling properties.

Experimental section

Materials. All chemicals were purchased from Sigma-Aldrich and used as received unless noted otherwise. Deionized water (DIW) with resistivity $>15 \text{ M}\Omega\cdot\text{cm}$ was obtained from Millipore Elix 3. 2-(dimethylamino)ethyl methacrylate (DMAEMA) was passed through an inhibitor removal column (Sigma-Aldrich) before any polymerizations. 11-(2-bromo-2-methyl)propionyloxy undecyl trichlorosilane (eBMPUS) was purchased from Gelest. Silicon wafers (p-doped, orientation $\langle 100 \rangle$) were purchased from Silicon Valley Microelectronics.

Sample preparation

Polymer brush formation. We prepared substrates grafted with PDMAEMA by utilizing surface-initiated atom transfer radical polymerization (SI-ATRP). Silicon wafers (12 mm × 40 mm) were exposed to ultraviolet/ozone treatment (UVO, Model 42, Jelight Co.) for 30 min before use. The silane initiator (11-(2-bromo-2-methyl)propionyloxyundecyl trichlorosilane, eBMPUS) was deposited on the silicon wafer by incubating in a solution (0.005% v/v of eBMPUS in hexanes) at room temperature for 48 hr. The ATRP solution containing DMAEMA (4 mL, 23.7 mM), DIW (36.8 mL, 2.0442 M), and isopropanol (9.2 mL, 120.3 mM) was prepared in a 150 mL round-bottom flask. The solution was purged with argon gas for 10 min. The ligand 2,2'-bipyridine (0.1421 g, 0.9 mM) and the catalyst CuCl (0.03917 g, 0.4 mM) were added to the solution; the solution was mixed using a stir-bar and was degassed by blowing argon gas for 15 min. The PDMAEMA grafts were obtained by placing the initiator-coated substrates in a 20 mL vial filled with the ATRP solution for 120 min at room temperature.

SI-ATRP formed poly (2-(methacryloyloxy)ethyl-trimethylammonium chloride) (PMETAC) brushes. The ATRP solution contained [METAC]:[CuCl]:[2,2'-bipyridine]=[60]:[1]:[2.3]. The METAC monomer (11.46 mL, 60.1 mM) was with DIW (3.9 mL, 0.2163 M) and IPA (14.6 mL, 0.1916 M). The polymerization was carried out at room temperature for 5 hr. The resulting dry brush thickness was ~80 nm measured at 100 °C. For the poly(sulfobetaine methacrylate) (PSBMA) brushes, the ATRP solution was prepared with the molar ratio of [SBMA]:[CuBr]:[2,2'-bipyridine]=[25]:[1]:[2]. 3.02g (0.01 M) of monomer was dissolved into the mixed solvent of DIW (5 mL, 0.2778 M) and methanol (15 mL, 0.1962 M). The SI-ATRP was performed at 60 °C for 24 hr. The resulting dry brush thickness was ~90 nm measured at 100 °C.

Quaternization gradient of PDMAEMA. The PDMAEMA brushes were quaternized on a silicon substrate (6 mm × 40 mm) in the gaseous phase. The PDMAEMA brushes were placed vertically in an empty 10 ml glass beaker (inner diameter 2.5 cm, height 2.8 cm). 50 µL of 3.2 M methyl iodide-ethanol solution was injected into the beaker. After desired reaction time (*e.g.*, 120 sec), the specimen was removed from the beaker, rinsed with methanol, and dried with nitrogen gas.

Betainization of PDMAEMA. For the gaseous phase modification, 20 µl of 0.1 M 1,3-propanesultone (P-S) in ethanol was injected in an air-tight glass tube where PDMAEMA brushes or qPDMAEMA brushes sample was located. The glass tube was heated at 60°C for 30 min. Since

the volume of the reagent solution is small, most of it vaporized rapidly. The concentration of P-S and reaction time varied depending on the degree of betainization. After the reaction, the sample was incubated in 1 M NaCl aqueous solution for 20 min to remove any electrostatically adsorbed counterions. Finally, the sample was rinsed with DIW followed by drying with nitrogen gas flow. 7 mL of 0.1 M P-S solution in ethanol was utilized to immerse the entire sample substrate in the reagent solution for the liquid phase modification. The remaining procedures were identical.

Bacterial culture, growth conditions. *Escherichia coli* (*E. coli*) DH52 was obtained from the American Type Culture Collection (ATCC). For the bacterial experiments, bacteria cultures were grown on Luria-Bertani (LB) agar overnight at 37°C. Bacterial cells were collected from the culture via an inoculation loop and suspended in LB broths. The optical density at 600 nm (OD₆₀₀) of the bacterial suspensions was then adjusted to 0.3. The substrate was submerged in 3 mL of a bacterial suspension in 24-well plates. The substrate was incubated at 25°C in dark conditions and for 3 hr.

Characterization

Ellipsometry measurements. We utilized variable angle spectroscopic ellipsometry (VASE) (J.A. Woollam Co.) to measure polymer thin film thickness and refractive index. All samples were characterized using VASE at 100°C with two angles of incidence (60 and 65° relative to the normal) and the wavelength ranging from 400 to 800 nm.³⁴ A hot stage (FP82HT, Mettler Toledo) connected to a central processor (FP90, Mettler Toledo) was placed on the VASE sample stage to carry out the high-temperature ellipsometry measurements. We analyzed the ellipsometry data with WVASE32 software (J.A. Woollam Co.). Single Cauchy layer model for polymers ($n = A_n + B_n/\lambda^2$, where n is the refractive index and A_n (= 1.46-1.53) and B_n (= 0.005-0.009 μm^2) are the fitting parameters) on top of 1.5 nm SiO_x layer and Si substrate was used to fit the experimental data.

FTIR measurements. Fourier-transform infrared spectroscopy (FTIR) data were collected by performing 128 scans with 4 cm⁻¹ resolution in attenuated total reflection (ATR) mode with Ge crystal on a Nicolet 6700 spectrometer and analyzed using OMNIC software. All spectra have been processed by advanced ATR correction followed by baseline correction.

Confocal laser scanning microscopy measurements and data analysis. Confocal laser scanning microscopy (CLSM) was performed on a Leica SP8 inverted microscope. Washed biofilms were fluorescently stained with a Viability/Cytotoxicity Assay Kit for Bacteria Live & Dead Cells (Biotum, CA, USA). The kit includes DMAO and ethidium homodimer III (EthD-III). DMAO is a green-fluorescent nucleic acid dye that stains both live and dead bacteria. EthD-III is a red-fluorescent dye that selectively stains the dead cells with damaged cell membranes. Image J was employed to extract the green and red images from the raw CLSM files. These image files were further analyzed using the CellC Cell Counting software.³⁵ Comparing the numbers of green (live) and red (dead) cells estimates the cell viability on the investigated substrates.

Results and discussions

We studied the betainization of PDMAEMA brushes in the liquid and vapor phases.²⁴ In ethanol solution, P-S hydrolyzes, and the resulting sulfonic acid may protonate the repeat units of PDMAEMA and generate quaternary ammonium. The quaternary ammonium may, in turn, form ionic complexes with sulfonate groups in 3-ethoxypropanesulfonate, as shown in **Figure 1**. Therefore, we used betainization in the gaseous phase, using the procedures described in the Experimental section.^{31,32} This approach avoids hydrolyzation of P-S.

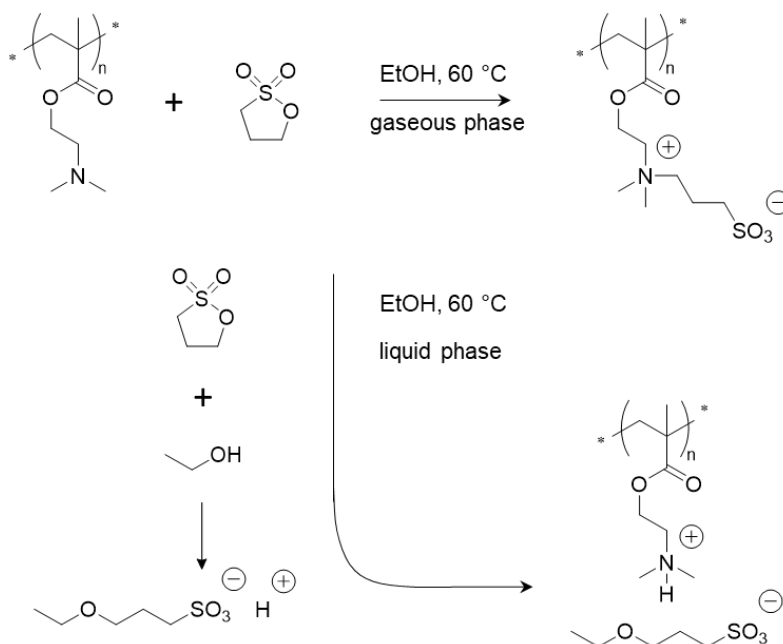


Figure 1. Reaction of PDMAEMA with 1,3-propanesultone in ethanol at 60°C. In a liquid phase reaction, the main products are the protonated PDMAEMA and 3-ethoxypropanesulfonate (undesired). In gaseous phase reaction, the main product is the betainized PDMAEMA (desired).

We carried out FTIR experiments to follow betainization in both liquid and vapor phases. **Figure 2** plots FTIR-ATR spectra for PDMAEMA brushes after different treatments. When the PDMAEMA brushes get protonated (pPDMAEMA), broad O-H stretching bands appear at ~ 3300 - 3700 cm^{-1} primarily due to water absorption. Also, the C-H stretching bands at ~ 2775 and $\sim 2825\text{ cm}^{-1}$ disappear, and we observe two small broad bands at ~ 2481 and $\sim 2701\text{ cm}^{-1}$ compared to the parent PDMAEMA. After betainization in the liquid phase (PDMAEMA (l)), two bands appear in the spectrum at ~ 1191 and $\sim 1042\text{ cm}^{-1}$, corresponding to S=O stretching and SO_3^- stretching, respectively. The modified brushes were incubated in 1 M of NaCl solution for 20 min to remove any residual ionic complexes from the sample surfaces. The FTIR spectrum from a sample after betainization in the liquid phase and subsequent incubation in NaCl (PDMAEMA (l) + NaCl) does not contain the sulfonate bands (~ 1191 and $\sim 1042\text{ cm}^{-1}$); the PDMAEMA (l) + NaCl spectrum is identical to that of pPDMAEMA, implying betainization did not occur. FTIR spectrum collected from a sample that was betainized in the vapor phase (PDMAEMA (g)) does not change even after incubation in NaCl (PDMAEMA (g) + NaCl). Both spectra match that collected from poly(sulfobetaine methacrylate) (PSBMA) brushes.

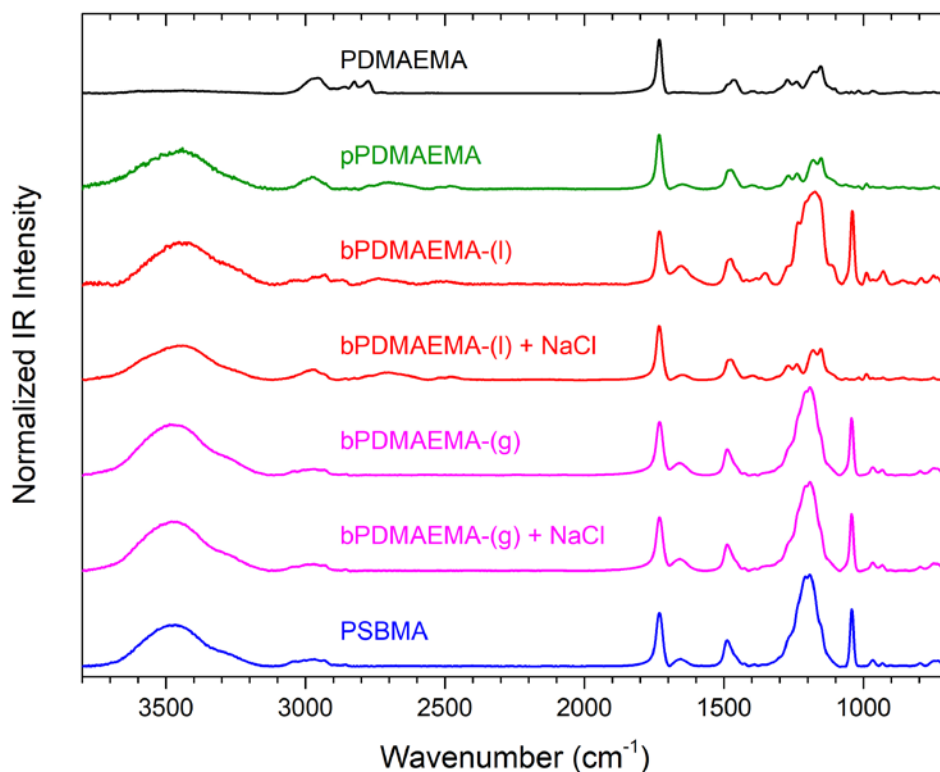


Figure 2. FTIR-ATR spectra (normalized to the carbonyl vibration at $\sim 1731\text{ cm}^{-1}$) collected from PDMAEMA, protonated PDMAEMA (pPDMAEMA), PDMAEMA betainized in the liquid phase

(PDMAEMA (l)), and vapor phase (PDMAEMA-(g)). PDMAEMA-(l) + NaCl and PDMAEMA-(g) + NaCl are spectra collected from PDMAEMA-(l) and PDMAEMA-(g) after incubation in NaCl solution.

Figure 3 displays the experimental procedure for fabricating the counter-propagating gradients (CPG) of quaternized and betainized polymer brushes. We prepared PDMAEMA brushes (~95 nm, dry thickness measured at 100°C) having comparable grafting density (assuming ~0.5 chains/nm²) and molecular weight (~150.8 kDa) from surface-initiated atom transfer radical polymerization (SI-ATRP).³⁶⁻³⁸ We gradually modified the PDMAEMA grafts spatially to various degrees of quaternization (DQ) by following the methodology outlined in our previous work.¹⁷ The gaseous phase quaternization involves four processes: i) evaporation of the quaternizing reagent (*i.e.*, MI), ii) diffusion of MI through the air, iii) diffusion of MI through polymer film, and iv) the reaction of MI with the polymer. The diffusion through the air is the rate-limiting step.¹⁷ The resulting surface features a number density gradient in the quaternized units. One can adjust gradient properties (*i.e.*, width and amplitude) by changing the MI solution concentration, the processing time, and the shape and size of the glass container for MI solution.

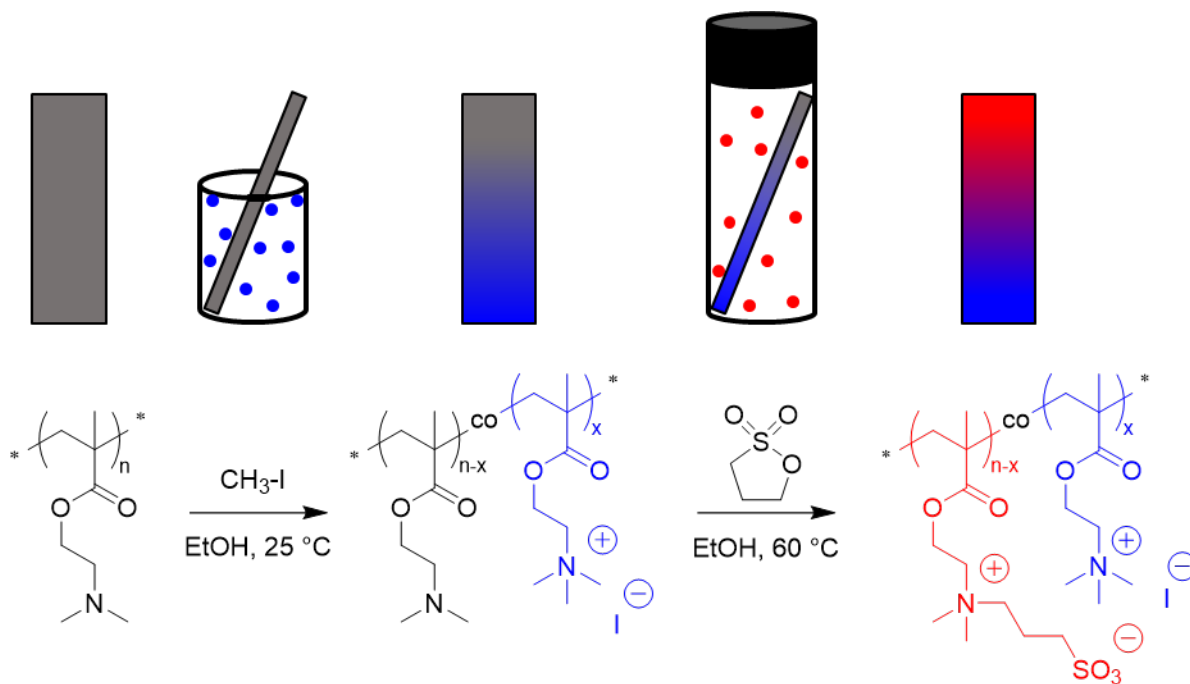


Figure 3. Post-polymerization modification processes for fabricating the counter-propagating gradients (CPG) of quaternized and betainized PDMAEMA brushes. Both quaternization and betainization are carried out in the gaseous phase.

In the subsequent step, we placed the quaternized specimens vertically in a glass reactor with 20 μ l of ethanol solution dissolving P-S at 60°C (closed-cap). P-S only reacts with the remaining tertiary amines in PDMAEMA but not the quaternary ammonium in qPDMAEMA (*cf.* **Figure S1**). The degree of modification can be controlled by the reaction time and P-S concentration (*cf.* **Figure S2**).

The resulting CPG sample was analyzed spatially with FTIR-ATR (*cf.* **Figure 4**). After baseline subtraction, every spectrum was normalized by the intensity at ~ 1731 cm^{-1} (the carbonyl group in the repeat units), which should remain unaffected by quaternization and betainization. Two distinct vibration bands, at ~ 956 and ~ 1042 cm^{-1} (blue and red bands in **Figure 4a**), were selected to determine the degree of quaternization (DQ) and degree of betainization (DB), respectively.^{17,39} To obtain the saturated intensities of both bands, 100 mol% quaternized and betainized brushes (PMETAC and PSBMA) were synthesized directly using SI-ATRP of the corresponding monomers. The normalized intensities at ~ 956 and ~ 1042 cm^{-1} were measured for various positions in the CPG sample. The DQ and DB values were determined using **Equations 1** and **2**:

$$DQ \text{ (mol\%)} = 100 \times \left[\frac{I_{\text{sample}} - I_{\text{PDMAEMA}}}{I_{\text{PMETAC}} - I_{\text{PDMAEMA}}} \right]_{956\text{cm}^{-1}} \quad (1)$$

$$DB \text{ (mol\%)} = 100 \times \left[\frac{I_{\text{sample}} - I_{\text{PDMAEMA}}}{I_{\text{PSBMA}} - I_{\text{PDMAEMA}}} \right]_{1042\text{cm}^{-1}} \quad (2)$$

In **Equations 1** and **2**, I_{PDMAEMA} , I_{PMETAC} , and I_{PSBMA} indicate the normalized intensity of PDMAEMA, PMETAC, and PSBMA at the corresponding wavenumbers. As demonstrated by the data in **Figure 4**, profiles of DQ and DB in the sample display counter-propagating character. The summation of the DQ and DB is ~ 100 mol%, implying that nearly all tertiary amines in the polymer repeat units got modified. Our previous work reported a maximum DQ of $\sim 85\%$, attributed to the polymer steric hindrance due to limited solubility. The complete modification of all tertiary amines in PDMAEMA after quaternization and betainization reactions may be due to a higher solubility of sulfobetaine in ethanol relative to that of quaternary ammonium. The DQ and total concentration obtained from FTIR can be verified by ellipsometry (*cf.* **Figure S3**).¹⁷

We confirm the complete betainization of PDMAEMA by exposing PDMAEMA brushes to P-S in ethanol at 60°C for various reaction times (*cf.* **Figure S2**). We used two P-S/ethanol solutions concentrations: 0.01 and 0.1 M. In both instances, full betainization was achieved in less

than ~30 min, which is very fast compared to reactions carried out in the liquid phase (usually 6~48 hr).^{15,31,32,40-43} We attribute the rapid kinetics of reactants to i) higher collision frequency and ii) little ionic complexation in the gaseous phase relative to that in the solution phase.

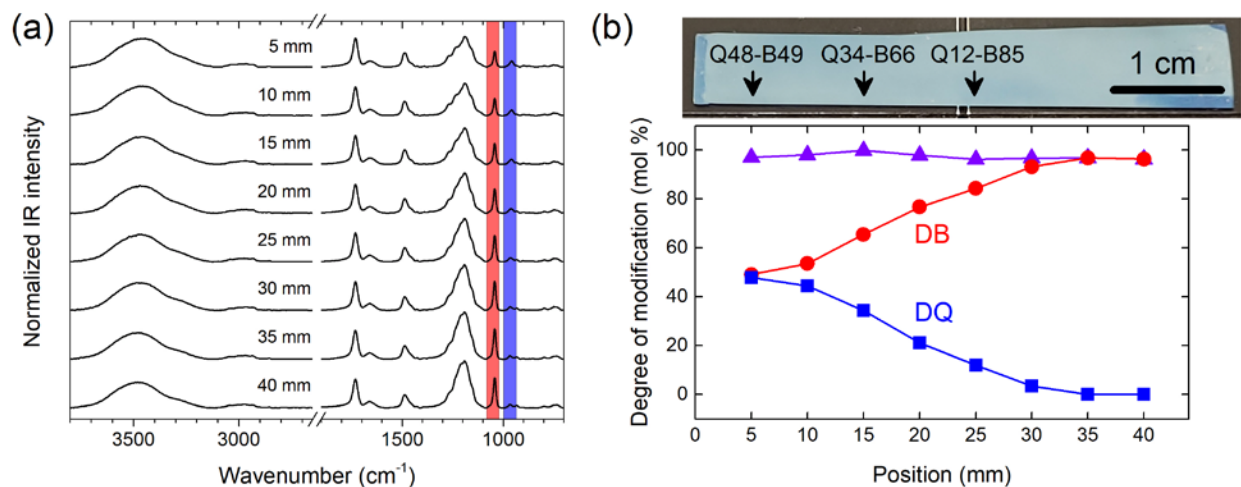


Figure 4. (a) FTIR-ATR spectra (normalized to the carbonyl vibration at $\sim 1731\text{ cm}^{-1}$) collected at different locations on the counter-propagating gradients of quaternized and betainized PDMAEMA brushes. The number above each spectrum denotes the distances from the "quaternized edge" of the sample. The bands at $\sim 1042\text{ cm}^{-1}$ (red) and $\sim 956\text{ cm}^{-1}$ (blue) represent the relative variation of the degree of betainization (DB) and degree of quaternization (DQ), respectively. (b) DQ (blue squares), DB (red circles), total (purple up-triangle) at various positions in the sample (measured from the "quaternized edge" of the sample). The scale bar corresponds to 1 cm.

The past few decades witnessed the development of several different types of antibacterial coatings. One of them involves quaternary amines with different lengths of the alkyl chain lengths.⁴⁴ A common problem with the antibacterial surface is that the dead bacterial cells remain attached to the surface after killing. Besides other complications, these cells block the active sites on the surface, which, in turn, loses its effectiveness. One way to address this issue is to make the coatings antifouling or remove the dead cells from the surface.^{42,45-47} Here, use the CPG surface to provide antibacterial and antifouling functions simultaneously. The surfaces of interest are at positions at 5, 15, 25, and 35 mm from the "quaternized edge" of the sample. The [DQ,DB] values at those positions are [48,49], [34,66], [12,85], and [0,97] and they are denoted as Q48-B49, Q34-B66, Q12-B85, and Q0-B97, respectively.

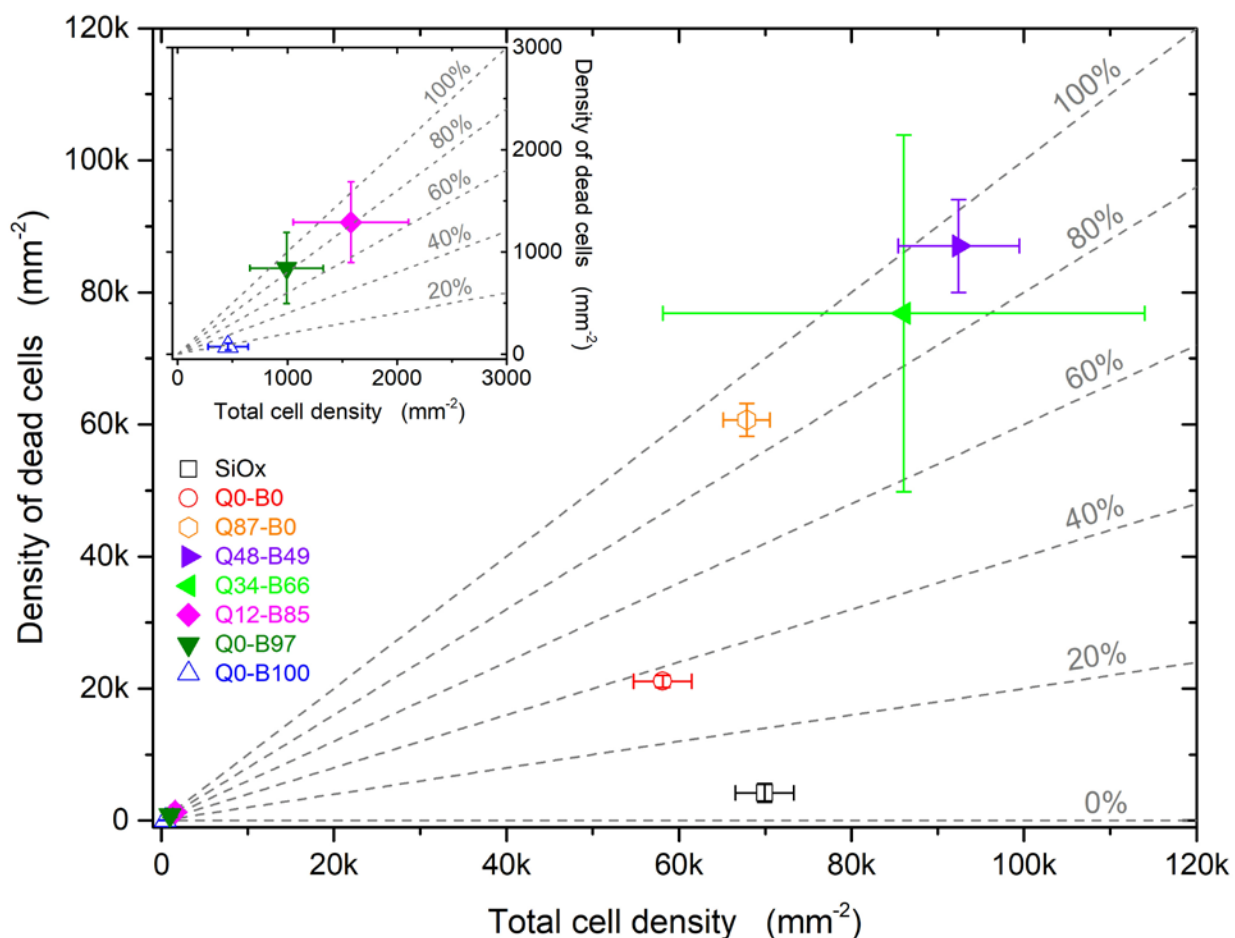
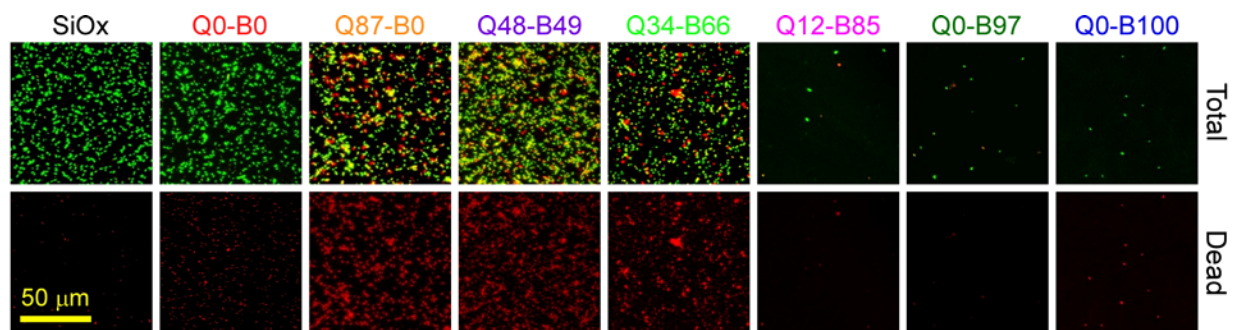


Figure 5. (top) Confocal microscope images of total cells and dead *E. coli* bacteria. The legend denotes the percentage of DQ and DB values. For example, Q48-B49 corresponds to 48 mol% and 49 mol% of DQ and DB at the position, respectively. Live and dead *E. coli* cells are shown in green and red colors, respectively. The scanning area is $\sim 100 \times 100 \mu\text{m}^2$. (bottom) The density of dead *E. coli* cells as a function of total adsorbed *E. coli* cells.

The CPG substrates were immersed in the suspension of *E. coli* and incubated for ~ 3 hr at 25°C . After staining with a Viability/Cytotoxicity Assay Kit for Bacteria Live & Dead Cells, the samples were imaged with CLSM and analyzed with CellC software. The dead cells appear red in the images, and the live cells display green in **Figure 5**. SiOx and PDMAEMA (Q0-B0) brushes

exhibit comparable total cell density without a noticeable bactericidal effect. Quaternized polymer brushes (Q87-B0) are antibacterial; they kill ~90 % of bacteria. Betainized brushes (Q0-B97, Q0-B100) exhibit antifouling behavior. The region at Q48-B49 exhibits mainly antibacterial function with killing above ~90% of bacteria. At the region of Q34-B66, only ~34 mol% of quaternary ammonium with methyl group killed ~90% of bacteria on the surface. Also, the total cell density decreased slightly with increasing the degree of betainization. In regions Q12-B85 and Q0-B97, the trend changes dramatically. The surface predominantly shows antifouling function; only a few cells can be observed in the images. Despite the limited data set, it is safe to conclude that surfaces between Q34-B66 and Q12-B85 exhibit the dual functionality of antibacterial and antifouling function concurrently.

In summary, we documented that betainization of PDMAEMA brushes using P-S proceeds more efficiently when carried out in the vapor phase (*i.e.*, evaporation of reagent solutions at 60°C) than in the liquid phase. When reacting in the vapor phase, P-S does not form ionic complexes with PDMAEMA. The betainization reaction (pseudo-first-order in P-S), conducted with P-S ethanolic solutions with 0.01 and 0.1 M concentrations, resulted in complete betainization of PDMAEMA in <30 min. We generated counter-propagating gradients (CPG) on PDMAEMA brushes by sequential and directional quaternization and betainization from the vapor phase. We established the degrees of quaternization (DQ) and betainization (DB) as a function of position on the sample using FTIR-ATR. We further employed the CPG substrates in studying antibacterial and antifouling behavior. While fully betainized samples exhibited antifouling behavior, specimens containing 12% of quaternized and 85% of betainized units acted simultaneously as antibacterial and antifouling surfaces.

Associated content

Supporting information

The Supporting Information is available free of charge on the ACS Publications website.

Ionic complexation between quaternary ammonium and sulfonate groups. Reaction kinetics of PDMAEMA betainization from the vapor phase. Quaternized and betainized counter-propagating gradients. The density of dead and live *E. coli* cells on the substrate. (PDF).

Author information

*Email: jgenzer@ncsu.edu

ORCID: Yeongun Ko: 0000-0001-5770-6707

ORCID: Vi Khanh Truong: 0000-0002-6016-6438

ORCID: Sun Young Woo: 0000-0002-3091-2479

ORCID: Michael Dickey: 0000-0003-1251-1871

ORCID: Lilian Hsiao; 0000-0002-4448-7397

ORCID: Jan Genzer: 0000-0002-1633-238X

Acknowledgment

The work was supported by the National Science Foundation, Grant no. DMR-1404639. We appreciate the partial support from the National Science Foundation, Grant no. DMR-1809453. Australian-American Fulbright Commission supported VKT.

References

- (1) Bhat, R. R.; Tomlinson, M. R.; Wu, T.; Genzer, J. Surface-Grafted Polymer Gradients: Formation, Characterization, and Applications. *Adv. Polym. Sci.* **2006**, *198*, 51–124.
- (2) Genzer, J.; Bhat, R. R. Surface-Bound Soft Matter Gradients. *Langmuir* **2008**, *24* (6), 2294–2317.
- (3) Genzer, J. Surface-Bound Gradients for Studies of Soft Materials Behavior. *Annu. Rev. Mater. Res.* **2012**, *42* (1), 435–468.
- (4) Schreiber, F. Structure and Growth of Self-Assembling Monolayers. *Prog. Surf. Sci.* **2000**, *65* (5), 151–257.
- (5) Pujari, S. P.; Scheres, L.; Marcelis, A. T. M.; Zuilhof, H. Covalent Surface Modification of Oxide Surfaces. *Angew. Chemie Int. Ed.* **2014**, *53* (25), 6322–6356.
- (6) Chen, W. L.; Cordero, R.; Tran, H.; Ober, C. K. 50th Anniversary Perspective: Polymer Brushes: Novel Surfaces for Future Materials. *Macromolecules* **2017**, *50* (11), 4089–4113.
- (7) Zoppe, J. O.; Ataman, N. C.; Mocny, P.; Wang, J.; Moraes, J.; Klok, H. A. Surface-Initiated Controlled Radical Polymerization: State-of-the-Art, Opportunities, and Challenges in Surface and Interface Engineering with Polymer Brushes. *Chem. Rev.* **2017**, *117* (3), 1105–1318.
- (8) Pyun, J.; Kowalewski, T.; Matyjaszewski, K. Synthesis of Polymer Brushes Using Atom Transfer Radical Polymerization. *Macromol. Rapid Commun.* **2003**, *24* (18), 1043–1059.
- (9) Divandari, M.; Trachsel, L.; Yan, W.; Rosenboom, J.-G.; Spencer, N. D.; Zenobi-Wong, M.; Morgese, G.; Ramakrishna, S. N.; Benetti, E. M. Surface Density Variation within Cyclic Polymer Brushes Reveals Topology Effects on Their Nanotribological and Biopassive Properties. *ACS Macro Lett.* **2018**, *7* (12), 1455–1460.
- (10) Divandari, M.; Morgese, G.; Trachsel, L.; Romio, M.; Dehghani, E. S.; Rosenboom, J.-G.; Paradisi, C.; Zenobi-Wong, M.; Ramakrishna, S. N.; Benetti, E. M. Topology Effects on the Structural and Physicochemical Properties of Polymer Brushes. *Macromolecules* **2017**, *50* (19), 7760–7769.
- (11) Galvin, C. J.; Genzer, J. Applications of Surface-Grafted Macromolecules Derived from

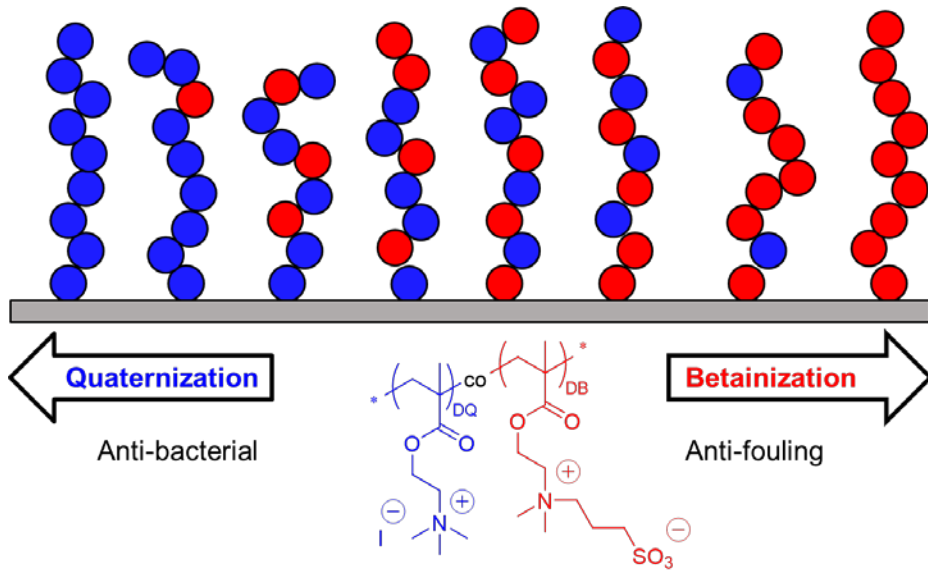
- Post-Polymerization Modification Reactions. *Prog. Polym. Sci.* **2012**, *37* (7), 871–906.
- (12) Günay, K. A.; Theato, P.; Klok, H.-A. Standing on the Shoulders of Hermann Staudinger: Post-Polymerization Modification from Past to Present. *J. Polym. Sci. Part A Polym. Chem.* **2013**, *51* (1), 1–28.
- (13) Das, A.; Theato, P. Activated Ester Containing Polymers: Opportunities and Challenges for the Design of Functional Macromolecules. *Chem. Rev.* **2016**, *116* (3), 1434–1495.
- (14) Gauthier, M. A.; Gibson, M. I.; Klok, H.-A. Synthesis of Functional Polymers by Post-Polymerization Modification. *Angew. Chemie Int. Ed.* **2009**, *48* (1), 48–58.
- (15) Song, L.; Lam, Y. M. Selective Betainization of PS–P4VP and Solution Properties. *Langmuir* **2006**, *22* (1), 319–324.
- (16) Jhon, Y. K.; Semler, J. J.; Genzer, J. Effect of Solvent Quality and Chain Confinement on the Kinetics of Polystyrene Bromination. *Macromolecules* **2008**, *41* (18), 6719–6727.
- (17) Ko, Y.; Christau, S.; Von Klitzing, R.; Genzer, J. Charge Density Gradients of Polymer Thin Film by Gaseous Phase Quaternization. *ACS Macro Lett.* **2020**, *9* (2), 158–162.
- (18) Barbey, R.; Laporte, V.; Alnabulsi, S.; Klok, H.-A. Postpolymerization Modification of Poly(Glycidyl Methacrylate) Brushes: An XPS Depth-Profiling Study. *Macromolecules* **2013**, *46* (15), 6151–6158.
- (19) Arifuzzaman, S.; Özçam, A. E.; Efimenko, K.; Fischer, D. A.; Genzer, J. Formation of Surface-Grafted Polymeric Amphiphilic Coatings Comprising Ethylene Glycol and Fluorinated Groups and Their Response to Protein Adsorption. *Biointerphases* **2009**, *4* (2), FA33–FA44.
- (20) Pandiyarajan, C. K.; Rubinstein, M.; Genzer, J. Surface-Anchored Poly(N-Isopropylacrylamide) Orthogonal Gradient Networks. *Macromolecules* **2016**, *49* (14), 5076–5083.
- (21) Pandiyarajan, C. K.; Genzer, J. Thermally Activated One-Pot, Simultaneous Radical and Condensation Reactions Generate Surface-Anchored Network Layers from Common Polymers. *Macromolecules* **2019**, *52* (2), 700–707.
- (22) Pandiyarajan, C. K.; Genzer, J. UV- and Thermally-Active Bifunctional Gelators Create

- Surface-Anchored Polymer Networks. *Macromol. Rapid Commun.* **2021**, *42* (16), 2100266.
- (23) Paschke, S.; Lienkamp, K. Polyzwitterions: From Surface Properties and Bioactivity Profiles to Biomedical Applications. *ACS Appl. Polym. Mater.* **2020**, *2* (2), 129–151.
- (24) Fischer, R. F. Propanesultone. *Ind. Eng. Chem.* **1964**, *56* (3), 41–45.
- (25) Rawlinson, L.-A. B.; Ryan, S. M.; Mantovani, G.; Syrett, J. A.; Haddleton, D. M.; Brayden, D. J. Antibacterial Effects of Poly(2-(Dimethylamino Ethyl)Methacrylate) against Selected Gram-Positive and Gram-Negative Bacteria. *Biomacromolecules* **2010**, *11* (2), 443–453.
- (26) Bowen, L.; Priyesh, J.; Jinrong, M.; K., S. J.; Zhefan, Y.; Hsiang-Chieh, H.; Yuwei, H.; Xiaojie, L.; Kan, W.; Jim, P.; Shaoyi, J. Trimethylamine N-Oxide–Derived Zwitterionic Polymers: A New Class of Ultralow Fouling Bioinspired Materials. *Sci. Adv.* **2021**, *5* (6), eaaw9562.
- (27) Schlenoff, J. B. Zwitteration: Coating Surfaces with Zwitterionic Functionality to Reduce Nonspecific Adsorption. *Langmuir* **2014**, *30* (32), 9625–9636.
- (28) Laschewsky, A.; Rosenhahn, A. Molecular Design of Zwitterionic Polymer Interfaces: Searching for the Difference. *Langmuir* **2019**, *35* (5), 1056–1071.
- (29) Baggerman, J.; Smulders, M. M. J.; Zuilhof, H. Romantic Surfaces: A Systematic Overview of Stable, Biospecific, and Antifouling Zwitterionic Surfaces. *Langmuir* **2019**, *35* (5), 1072–1084.
- (30) Jiang, S.; Ishihara, K.; Iwasaki, Y.; Vancso, J. Zwitterionic Interfaces: Concepts and Emerging Applications Special Issue. *Langmuir* **2019**, *35* (5), 1055.
- (31) Yang, R.; Xu, J.; Ozaydin-Ince, G.; Wong, S. Y.; Gleason, K. K. Surface-Tethered Zwitterionic Ultrathin Antifouling Coatings on Reverse Osmosis Membranes by Initiated Chemical Vapor Deposition. *Chem. Mater.* **2011**, *23* (5), 1263–1272.
- (32) Yang, R.; Gleason, K. K. Ultrathin Antifouling Coatings with Stable Surface Zwitterionic Functionality by Initiated Chemical Vapor Deposition (ICVD). *Langmuir* **2012**, *28* (33), 12266–12274.

- (33) Hart, R.; Timmerman, D. New Polyampholytes: The Polysulfobetaines. *J. Polym. Sci.* **1958**, *28* (118), 638–640.
- (34) Ko, Y.; Miles, J. R.; Genzer, J. Determining Water Sorption and Desorption in Thin Hydrophilic Polymer Films by Thermal Treatment. *ACS Appl. Polym. Mater.* **2019**, *1* (9), 2495–2502.
- (35) Selinummi, J.; Seppälä, J.; Yli-Harja, O.; Puhakka, J. A. Software for Quantification of Labeled Bacteria from Digital Microscope Images by Automated Image Analysis. *Biotechniques* **2005**, *39* (6), 859–863.
- (36) Patil, R. R.; Turgman-Cohen, S.; Šrogl, J.; Kiserow, D.; Genzer, J. On-Demand Degrafting and the Study of Molecular Weight and Grafting Density of Poly(Methyl Methacrylate) Brushes on Flat Silica Substrates. *Langmuir* **2015**, *31* (8), 2372–2381.
- (37) Patil, R. R.; Turgman-Cohen, S.; Šrogl, J.; Kiserow, D.; Genzer, J. Direct Measurement of Molecular Weight and Grafting Density by Controlled and Quantitative Degrafting of Surface-Anchored Poly(Methyl Methacrylate). *ACS Macro Lett.* **2015**, *4* (2), 251–254.
- (38) Ko, Y.; Miles, J. R.; Genzer, J. Determining Water Sorption and Desorption in Thin Hydrophilic Polymer Films by Thermal Treatment. *ACS Appl. Polym. Mater.* **2019**, *1* (9), 2495–2502.
- (39) Walker, E. J.; Pandiyarajan, C. K.; Efimenko, K.; Genzer, J. Generating Surface-Anchored Zwitterionic Networks and Studying Their Resistance to Bovine Serum Albumin Adsorption. *ACS Appl. Polym. Mater.* **2019**, *1* (12), 3323–3333.
- (40) Bütün, V. Selective Betainization of 2-(Dimethylamino)Ethyl Methacrylate Residues in Tertiary Amine Methacrylate Diblock Copolymers and Their Aqueous Solution Properties. *Polymer* **2003**, *44* (24), 7321–7334.
- (41) Pei, Y.; Lowe, A. B. Polymerization-Induced Self-Assembly: Ethanolic RAFT Dispersion Polymerization of 2-Phenylethyl Methacrylate. *Polym. Chem.* **2014**, *5* (7), 2342–2351.
- (42) Widyaya, V. T.; Müller, C.; Al-Ahmad, A.; Lienkamp, K. Three-Dimensional, Bifunctional Microstructured Polymer Hydrogels Made from Polyzwitterions and Antimicrobial Polymers. *Langmuir* **2019**, *35* (5), 1211–1226.

- (43) Zhang, C.; Yin, C.; Wang, Y.; Zhou, J.; Wang, Y. Simultaneous Zwitterionization and Selective Swelling-Induced Pore Generation of Block Copolymers for Antifouling Ultrafiltration Membranes. *J. Memb. Sci.* **2020**, *599*, 117833.
- (44) Koufakis, E.; Manouras, T.; Anastasiadis, S. H.; Vamvakaki, M. Film Properties and Antimicrobial Efficacy of Quaternized PDMAEMA Brushes: Short vs Long Alkyl Chain Length. *Langmuir* **2020**, *36* (13), 3482–3493.
- (45) Lv, J.; Jin, J.; Chen, J.; Cai, B.; Jiang, W. Antifouling and Antibacterial Properties Constructed by Quaternary Ammonium and Benzyl Ester Derived from Lysine Methacrylamide. *ACS Appl. Mater. Interfaces* **2019**, *11* (28), 25556–25568.
- (46) Liu, T.; Yan, S.; Zhou, R.; Zhang, X.; Yang, H.; Yan, Q.; Yang, R.; Luan, S. Self-Adaptive Antibacterial Coating for Universal Polymeric Substrates Based on a Micrometer-Scale Hierarchical Polymer Brush System. *ACS Appl. Mater. Interfaces* **2020**, *12* (38), 42576–42585.
- (47) Zou, Y.; Zhang, Y.; Yu, Q.; Chen, H. Dual-Function Antibacterial Surfaces to Resist and Kill Bacteria: Painting a Picture with Two Brushes Simultaneously. *J. Mater. Sci. Technol.* **2021**, *70*, 24–38.

TOC Figure



Supporting Information

Counter-propagating gradients of antibacterial and antifouling polymer brushes

Yeongun Ko^{1,†}, Vi Khanh Truong^{1,2}, Sun Young Woo¹, Michael D. Dickey¹, Lilian Hsiao¹,
Jan Genzer^{1,3,*}

¹ Department of Chemical and Biomolecular Engineering
North Carolina State University
Raleigh, NC 27695-7905, USA

² Nanobiotechnology Laboratory, School of Science
RMIT University
Melbourne, VIC 3000, Australia

³ Global Station for Soft Matter, Global Institution for Collaborative Research and Education
(GI-CoRE)
Hokkaido University
Hokkaido 060-0808, Japan

We wanted to verify ionic complexation between the quaternary ammonium and sulfonate groups. We synthesized poly(2-methacryloyloxyethyltrimethylammonium chloride) (PMETAC) brushes containing 100 mol% quaternized repeat units, *i.e.*, betainization should not occur. After incubation in 1,3-propanesulfonate ethanol solution for 30 mins, we observe strong bands at ~ 1192 and ~ 1042 cm^{-1} in the IR spectrum (*cf.* **Figure S1**), corresponding to the asymmetric S=O stretching and SO_3^- stretching, respectively (PMETAC-(1)).^{1,2} The presence of the signals does not necessarily support the betainization because the 3-ethoxypropanesulfonate can exist as counter ions of quaternary ammonium without the betainization. Indeed, after incubation in 1 M of NaCl aqueous solution, the signals related to sulfonate disappeared (PMETAC-(1) + NaCl). It is because the external Cl exchanged the 3-ethoxypropanesulfonate counter ions. The result clearly shows that there is no modification at the repeat units of PMETAC brushes.

[†] Present address: Department of Chemical Engineering, University of Michigan, Ann Arbor, MI 48109-2800

* Corresponding author: jgenzer@ncsu.edu

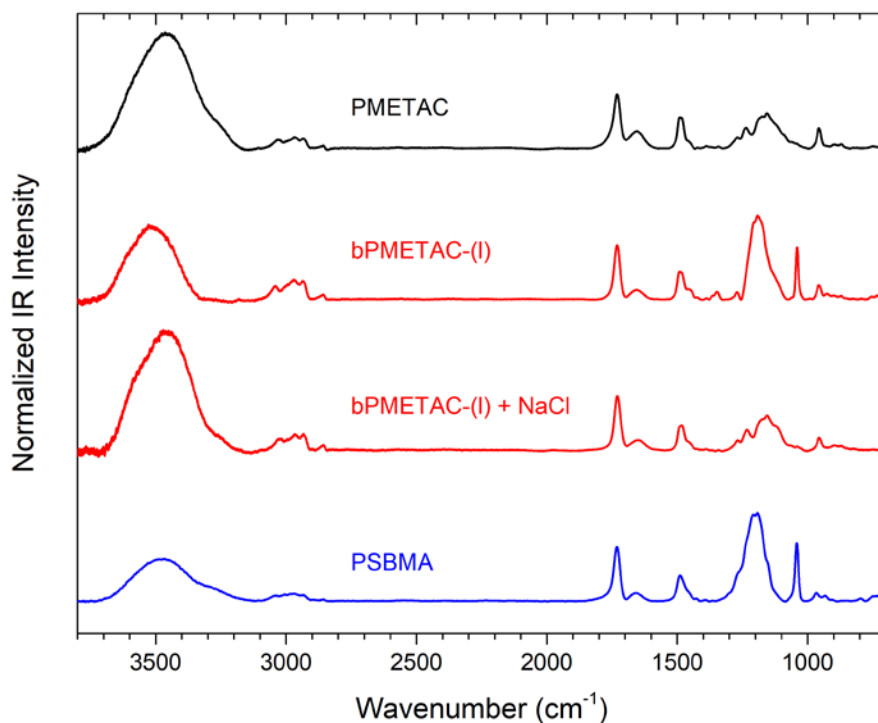


Figure S1. FTIR-ATR spectra (normalized to the carbonyl vibration at $\sim 1731\text{ cm}^{-1}$) of PMETAC brushes with different treatments. The native PMETAC brushes were incubated in 0.1 M of 1,3-propanesultone ethanol solution at 60°C for 30 mins (PMETAC-(I)). The betainized sample was placed in 1 M of NaCl aqueous solution for 20 mins (PMETAC-(I) + NaCl). For the comparison, we display the FTIR spectrum collected from PSBMA brushes.

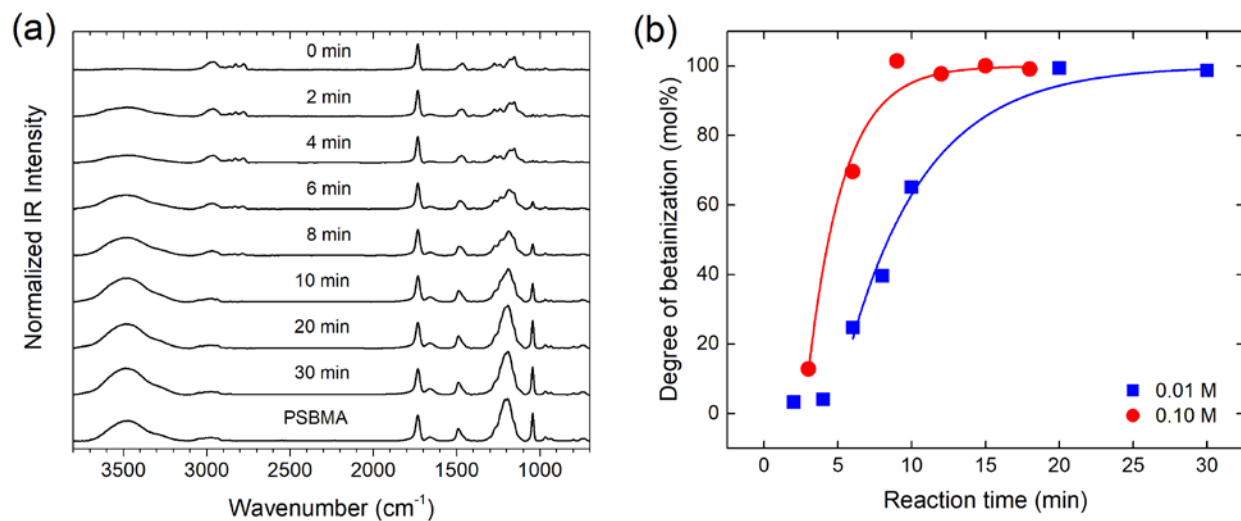


Figure S2. (a) FTIR spectra (normalized to the carbonyl vibration at $\sim 1731\text{ cm}^{-1}$) of betainized PDMAEMA brushes with different reaction times in the vapor phase conducting by evaporation P-S from 0.01 M solutions of P-S in ethanol at 60°C . (b) Degree of betainization of PDMAEMA brushes obtained by betainization from vapor phase using P-S solutions in ethanol (P-S concentrations 0.01 and 0.1 M, 60°C) for various reaction times.

FTIR-ATR monitors the kinetics of the betainization reaction (*cf.* **Figure S2**). With increasing reaction time, the C-H stretching bands at ~ 2775 and ~ 2825 cm^{-1} get suppressed. Concurrently the O-H bands ~ 3300 - 3600 cm^{-1} and sulfonate bands ~ 1190 and ~ 1042 cm^{-1} increase in intensity (*cf.* **Figure S2a**). All samples were incubated in a 1 M NaCl aqueous solution to remove any ionic complexes before measuring the FTIR. By utilizing the band intensity at ~ 1042 cm^{-1} , we estimate the degree of betainization (DB) using **Equation 2** (*cf.* **Figure S2b**). At 0.1 M P-S, the DB reached up to 100 mol% within 15 mins, which is much faster than other reported reaction times (6-48 hrs).³⁻⁹ The results were fitted by pseudo-first-order reaction kinetics with the rate constants of 0.0031 and 0.0069 s^{-1} for 0.01 and 0.1 M of P-S in ethanol, respectively.

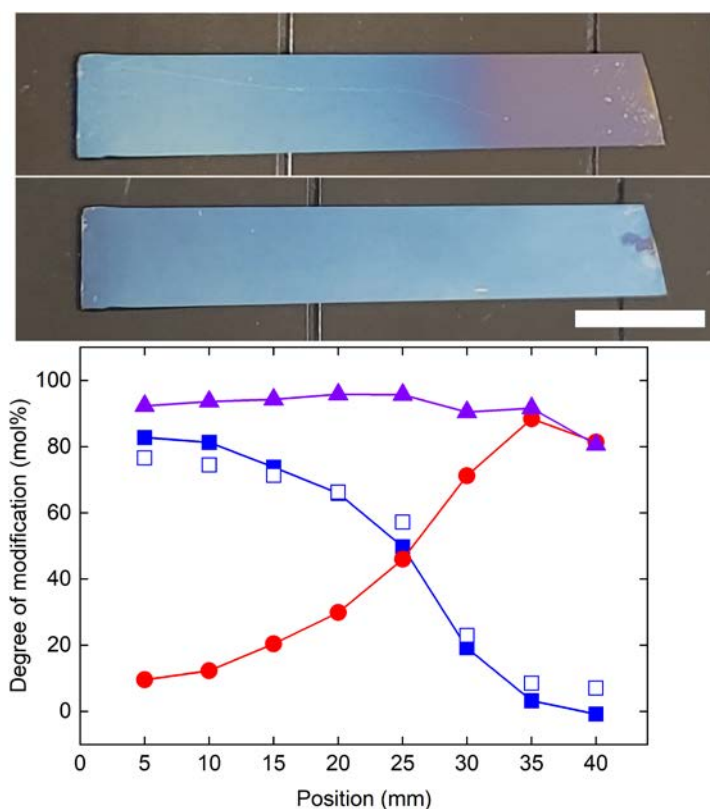


Figure S3. Degree of modifications as a function of the position of the PDMAEMA brush substrate. Corresponding photographs of the samples after quaternization (top) and subsequent betainization (bottom) are shown above the graph. The scale bar is 1 cm. In the graph, the solid red circles, blue squares, and purple triangles indicate DQ, DB, and the sum of DB and DQ, respectively, as obtained from FTIR. The open symbols correspond to the data obtained from ellipsometry.

Counter-propagating gradients were characterized by both FTIR-ATR and ellipsometry (**Figure S3**). Normalized IR intensities at ~ 956 and ~ 1042 cm^{-1} were converted into DQ and DB, respectively, using **Equation 1** and **2** in the manuscript. Ellipsometry measurement can further confirm

the DQ values as discussed in previous work.¹⁰ **Figure S3** shows a good agreement of DQ values from both FTIR-ATR and ellipsometry. In addition, the fact that the sum of DQ and DB is nearly 100 mol% supports the accuracy of characterization.

References

- (1) Shivapooja, P.; Yu, Q.; Orihuela, B.; Mays, R.; Rittschof, D.; Genzer, J.; López, G. P. Modification of Silicone Elastomer Surfaces with Zwitterionic Polymers: Short-Term Fouling Resistance and Triggered Biofouling Release. *ACS Appl. Mater. Interfaces* **2015**, *7* (46), 25586–25591.
- (2) Walker, E. J.; Pandiyarajan, C. K.; Efimenko, K.; Genzer, J. Generating Surface-Anchored Zwitterionic Networks and Studying Their Resistance to Bovine Serum Albumin Adsorption. *ACS Appl. Polym. Mater.* **2019**, *1* (12), 3323–3333.
- (3) Bütün, V. Selective Betainization of 2-(Dimethylamino)Ethyl Methacrylate Residues in Tertiary Amine Methacrylate Diblock Copolymers and Their Aqueous Solution Properties. *Polymer* **2003**, *44* (24), 7321–7334.
- (4) Song, L.; Lam, Y. M. Selective Betainization of PS–P4VP and Solution Properties. *Langmuir* **2006**, *22* (1), 319–324.
- (5) Yang, R.; Xu, J.; Ozaydin-Ince, G.; Wong, S. Y.; Gleason, K. K. Surface-Tethered Zwitterionic Ultrathin Antifouling Coatings on Reverse Osmosis Membranes by Initiated Chemical Vapor Deposition. *Chem. Mater.* **2011**, *23* (5), 1263–1272.
- (6) Yang, R.; Gleason, K. K. Ultrathin Antifouling Coatings with Stable Surface Zwitterionic Functionality by Initiated Chemical Vapor Deposition (ICVD). *Langmuir* **2012**, *28* (33), 12266–12274.
- (7) Pei, Y.; Lowe, A. B. Polymerization-Induced Self-Assembly: Ethanolic RAFT Dispersion Polymerization of 2-Phenylethyl Methacrylate. *Polym. Chem.* **2014**, *5* (7), 2342–2351.
- (8) Widyaya, V. T.; Müller, C.; Al-Ahmad, A.; Lienkamp, K. Three-Dimensional, Bifunctional Microstructured Polymer Hydrogels Made from Polyzwitterions and Antimicrobial Polymers. *Langmuir* **2019**, *35* (5), 1211–1226.
- (9) Zhang, C.; Yin, C.; Wang, Y.; Zhou, J.; Wang, Y. Simultaneous Zwitterionization and Selective Swelling-Induced Pore Generation of Block Copolymers for Antifouling Ultrafiltration Membranes. *J. Memb. Sci.* **2020**, *599*, 117833.
- (10) Ko, Y.; Miles, J. R.; Genzer, J. Determining Water Sorption and Desorption in Thin Hydrophilic Polymer Films by Thermal Treatment. *ACS Appl. Polym. Mater.* **2019**, *1* (9), 2495–2502.
- (11) Ko, Y.; Genzer, J. Spontaneous Degrafting of Weak and Strong Polycationic Brushes in Aqueous Buffer Solutions. *Macromolecules* **2019**, *52* (16), 6192–6200.